ELL2 and EAF2 co-regulation of AKT in prostate cancer cells

Laura E. Pascal[1], Mingming Zhong[1], Erdong Cheng[1], Khalid Z. Masoodi[1], Wei Chen[1], Anthony Green[2], Brian W. Cross[1], Erica Parrinello[1], Lora H. Rigatti[3], and Zhou Wang[1,4,5]

[1]Department of Urology, University of Pittsburgh School of Medicine, Pittsburgh, PA, USA, [2]Department of Pathology, Pitt Biospecimen Core, University of Pittsburgh School of Medicine, Pittsburgh, PA, USA, [3]Division of Laboratory Animal Resources, University of Pittsburgh School of Medicine, Pittsburgh, PA 15216, USA, [4]University of Pittsburgh Cancer Institute, University of Pittsburgh School of Medicine, Pittsburgh, PA, USA [5]Department of Pharmacology and Chemical Biology, and University of Pittsburgh School of Medicine, Pittsburgh, PA, USA

Abstract

Elongation factor for RNA polymerase II 2 (ELL2) and ELL-associated factor 2 (EAF2) are two functionally related androgen responsive gene-encoded proteins with prostate tumor suppressor characteristics. EAF2 and ELL2 have both been shown to be down-regulated in advanced prostate cancer, and mice with either *Eaf2* or *Ell2* deficiency developed murine prostatic intraepithelial neoplasia (mPIN), increased cellular proliferation and increased vascularity. Functional studies have revealed that EAF2 and ELL2 can bind to each other and have similar roles in regulating cell proliferation, angiogenesis and prostate homeostasis. Here, cell line experiments showed that knockdown of EAF2 or ELL2 induced an increase in proliferation and migration in C4-2 and 22Rv1 prostate cancer cells. Concurrent knockdown of EAF2 and ELL2 increased proliferation and migration similarly to the loss of EAF2 or ELL2 alone. Mice with homozygous deletion of *Ell2* or heterozygous deletion of *Eaf2* developed mPIN lesions characterized by increased epithelial proliferation, intraductal microvessel density, and infiltrating intraductal CD3-positive T-cells compared to wild-type controls. Mice with combined heterozygous deletion of *Eaf2* and *Ell2* developed mPIN lesions that were similar to those observed in mice with deficiency in Eaf2 or Ell2 alone. These results suggest that EAF2 and ELL2 have similar functions and are likely to require each other in their regulation of prostate epithelial cell proliferation and migration in prostate cancer cells as well as their tumor suppressive properties in the murine prostate.

Figure 1. Cell proliferation in EAF2- and ELL2-deficient prostate cancer cells.

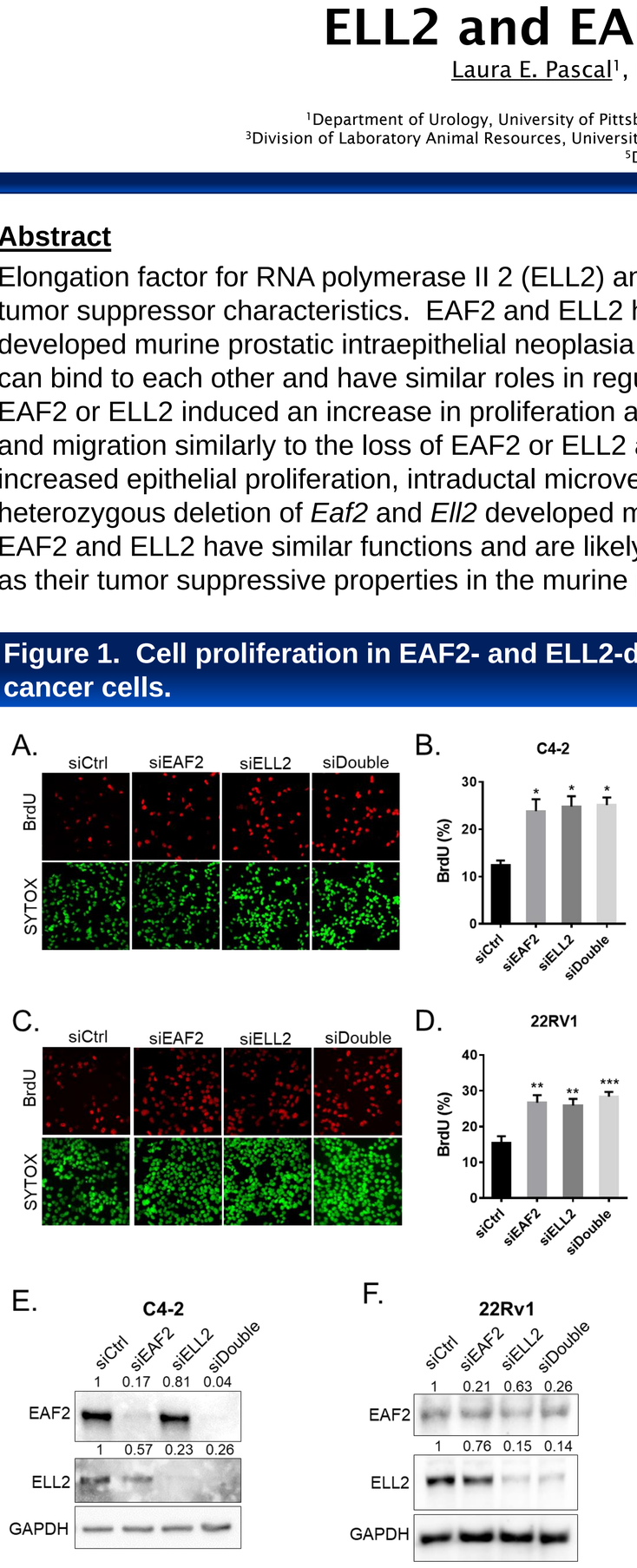

Figure 1. (A) BrdU incorporation in C4-2 cells transfected with siRNA, ×40. **(B)** Quantification of BrdU incorporation, mean percentage ± standard deviation of BrdU-positive cells relative to total number of cells. **(C)** BrdU incorporation in 22Rv1 cells. **(D)** Quantification of BrdU **(E)** Western blot analysis of EAF2 and ELL2 protein from C4-2 and **(F)** 22Rv1 cell lysates following siRNA knockdown. GAPDH served as internal loading control. *P < 0.05, **P < 0.01, ***P < 0.001.

Figure 2. Cell migration in EAF2- and ELL2-deficient prostate cancer cells.

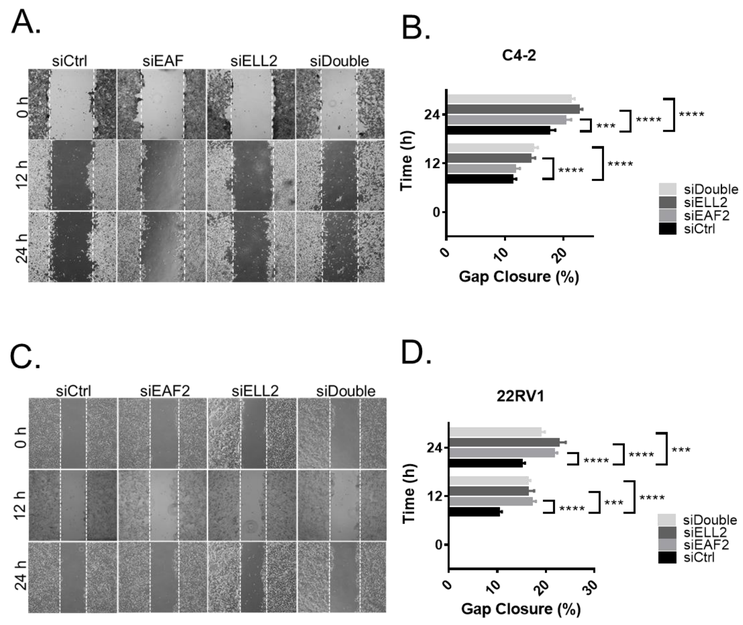

Figure 2. (A) Wound healing assay in C4-2 cells transfected with nontargeted siRNA. Cells were imaged at 0, 12, and 24 hours after treatment and gap widths were measured using ImageJ software (National Institutes of Health). Original magnification, ×10. **(B)** Quantification of gap closure in **A**, shown as the mean percentage ± standard error of the mean of initial gap. **(C)** Wound healing assay in 22Rv1 cells and **(D)** quantification of the images in **C**. Results are representative of three individual experiments. ***P < 0.001, ****P < 0.0001.

Figure 3. EAF2 and ELL2 co-regulated AKT in prostate cancer cells.

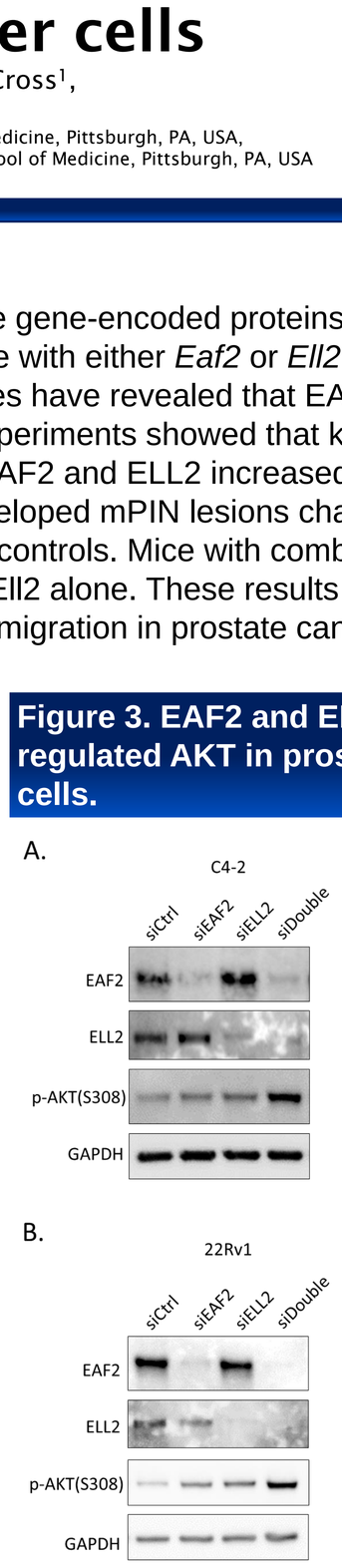

Figure 3. (A) Western blotting analysis of C4-2 cells transfected with nontargeted control (siCtrl) siRNA, targeted to EAF2 (siEAF2), ELL2 (siELL2), or concurrent EAF2 and ELL2 (siDouble) knockdown. **(B)** Western blotting analysis of 22Rv1 cells Results are representative of three individual experiments.

Concurrent EAF2 and ELL2 loss phenocopies individual EAF2 or ELL2 loss in prostate cancer cells and murine prostate

Figure 4. Combined loss of Eaf2 and Ell2 induced murine prostatic intraepithelial neoplasia in the mouse model

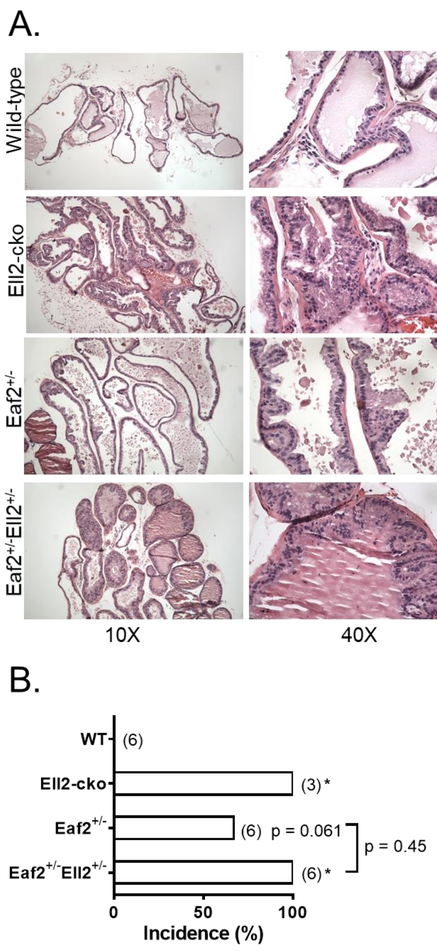

Figure 4. **(A)** Histology of mouse ventral prostate from C57BL/6J male mice with indicated genotype aged 24 mos stained with hematoxylin and eosin (H&E). **(B)** Quantification of mPIN incidence in mice. Data are expressed as percentage from 3 to 6 mice per group. *P < 0.05.

Figure 5. Effects of combined *Eaf2* and *Ell2* loss on epithelial proliferation in the C57BL/6J mouse prostate at age 24 mos.

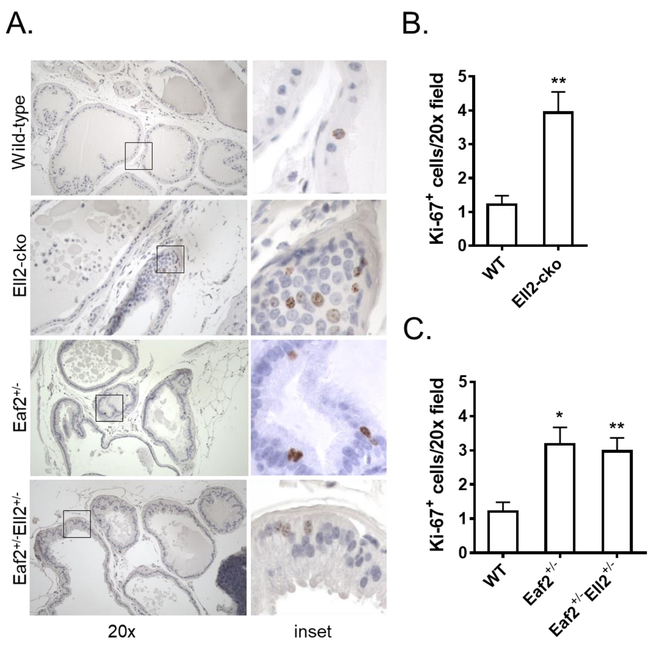

Figure 5. **(A**) Ki-67 immunostaining in transverse sections of prostate ventral lobes from indicated genotypes at 24 months of age. Original magnification, ×20. **(B)** Quantification of Ki-67+ epithelial cells in mouse prostate. **(C)** Quantification of Ki-67+ epithelial cells in mouse prostate from wild-type and *Ell2-cko* mice at 24 months of age. Data are expressed as mean ± standard error of the mean from 3 to 6 mice per group. *P < 0.05, **P < 0.01.

Figure 6. Effects of combined *Eaf2* and *Ell2* loss on CD31-positive microvessel density in the C57BL/6J mouse prostate at age 24 mos.

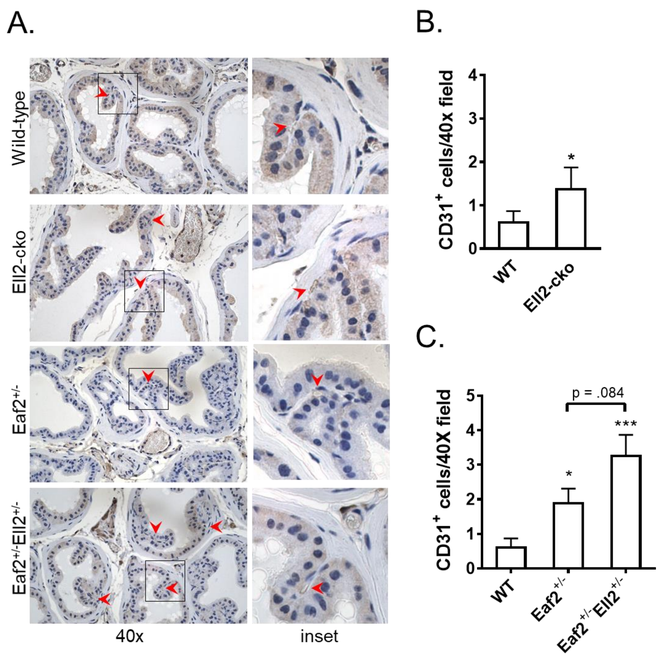

Figure 6. (A) CD31+ immunostaining in transverse sections of prostate dorsal-lateral lobes from indicated genotypes at 24 months of age. Red arrowheads indicate microvessel. Original magnification, ×40. **(B)** Quantification of CD31+ intraductal microvessels in mouse prostate from wild-type and Ell2-cko mice. **(C)** Quantification of CD31+ vessels in mouse prostate from wild-type and Ell2-cko mice. Data are expressed as mean ± standard error of the mean from 3 to 6 mice per group. *P < 0.05, ***P < 0.001.

Figure 7 Effects of combined *Eaf2* and *Ell2* loss on CD3-positive T cells in the C57BL/6J mouse prostate at age 24 mos.

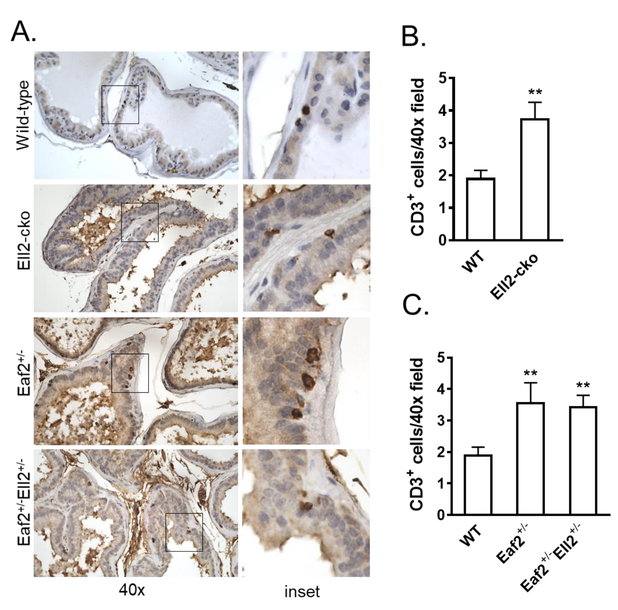

Figure 7. (A) CD3+ T cells immunostaining in transverse sections of prostate ventral lobes from indicated genotypes at 24 months of age. **(B)** Quantification of infiltrating intraductal CD3+ T cells in mouse prostate from wild-type and Ell2-cko mice at 24 months of age. **(C)** Quantification of CD3+ T cells in mouse prostate from wild-type and *Ell2-cko* mice at 24 months of age. Data are expressed as mean ± standard error of the mean from 3 to 6 mice per group. **P < 0.01.

Funding

This work was funded in part by National Institutes of Health Grants R01 CA186780 (Z.W.), P50 CA180995 (Z.W.), R50 CA211242 (L.E.P.), and T32 DK007774 (Z.W.) and scholarships from the Tippins Foundation (LEP) and the Mellam Foundation (KZM). This project used the UPCI Animal Facility and Tissue and Research Pathology Services (TARPS) and was supported in part by award P30CA047904.